Available online at www.sciencedirect.com
ScienceDirect
Journal of Molecular Catalysis A: Chemical 262 (2007) 36–40
JOURNAL OF MOLECULAR CATALYSIS A: CHEMICAL
www.elsevier.com/locate/molcata

Aerobic oxidation of *cis*-cyclooctene by iron-substituted polyoxotungstates: Evidence for a metal initiated auto-oxidation mechanism

Marcella Bonchio [a,*], Mauro Carraro [a], Anna Farinazzo [a], Andrea Sartorel [a], Gianfranco Scorrano [a], Ulrich Kortz [b]

[a] *ITM-CNR, University of Padova, Department of Chemical Sciences, Via Marzolo 1, 35131 Padova, Italy*
[b] *International University Bremen, School of Engineering and Science, P.O. Box 750 561, 28725 Bremen, Germany*

Available online 25 August 2006

Abstract

Catalytic aerobic epoxidation is a key process for new sustainable systems in the field of hydrocarbon functionalization. The screening of selected Fe-POM catalysts for the aerobic epoxidation has been performed using *cis*-cyclooctene as model substrate. Our results support a ubiquitous radical chain epoxidation with selectivity up to 66%, TOF in the range 4–50 h^{-1} and total turnover number >7000. FT-IR spectroscopy has been used to assess the stability of the various POM-based catalysts with respect to analogue organic porphyrine ligands.

Keywords: Polyoxometalates; Aerobic epoxidation; Iron; Catalytic oxidation; Oxygen

1. Introduction

Catalytic epoxidation using dioxygen as terminal oxidant represents a major goal of homogeneous catalysis [1]. The formation of epoxides via metal-catalyzed dioxygen activation is a key strategy for innovation and sustainability within industrial oxidation research [2]. However, in most of applied protocols, catalytic oxygenation requires harsh conditions of temperature and pressure or the use of additives as initiators and/or sacrificial co-reductants [1]. Moreover a general concern is the stability of the catalyst under turnover regime. In this respect, the adoption of a totally inorganic ligand system derived from polyoxometalates (POMs) represents a distinct advantage over coordination complexes displaying a set of organic ligands or organometallic moieties, susceptible to oxidative degradation [3–5]. POM ligands provide rigid and discrete metal-oxide frameworks with the general formula $[X_xM_mO_y]^{q-}$, where diversity can be generated by appropriate choice of metal addenda (M = Mo^{VI}, W^{VI}, etc.) and hetero atom (X), so that a formidable composition and structural variety is readily accessible [3–5]. Indeed, redox active transition metals, namely Fe, Ru, Mn, etc. can be incorporated within POM structures with different coordination geometries, in some cases, with striking analogies to oxygenase enzymes [6–8]. The synzyme analogy, and in particular a structural/catalysis parallelism with methane monooxygenase (MMO), has been recently invoked in the case of the di-iron substituted polyoxotungstate: γ-$[(FeOH_2)_2SiW_{10}O_{36}]^{6-}$ [9–11]. The latter has been found to mediate selective aerobic epoxidation, exhibiting dioxygenase activity, and unprecedented turnover number (TON = 10^4) albeit with a modest turnover frequency (TOF = 26 h^{-1}) [9]. A general problem, however, relies in the severe mechanistic complexity associated with metal-mediated aerobic oxidations, which hampers a precise understanding of the catalyst role [12]. Therefore, in most cases, the sought mechanistic adherence to bio-inspired guidelines is hardly envisaged. Herein, we report on the screening of selected Fe-POM catalysts for the aerobic epoxidation of *cis*-cyclooctene. Our results include: (i) structure–reactivity data based on the catalytic behavior of isostructural Krebs-type Fe complexes, (ii) kinetic and mechanistic evidence of a ubiquitous radical chain epoxidation with selectivity up to 66%, and (iii) TOF in the range 4–50 h^{-1} and total turnover number >7000. The stability of the various POM-based catalysts with respect to analogue porphyrin ligands will also be addressed.

* Corresponding author. Tel.: +39 049 827 5670; fax: +39 049 827 5239.
E-mail address: marcella.bonchio@unipd.it (M. Bonchio).

1381-1169/$ – see front matter © 2006 Elsevier B.V. All rights reserved.
doi:10.1016/j.molcata.2006.08.057

2. Experimental section

2.1. Materials

Fe-substituted polyoxotungstates were synthesized following literature procedures [13–15]. Li^+ salts were purified by gel permeation chromatography on Sephadex G50 column. Tetrahexylammonium (THA) salts were then obtained by cation metathesis in water. To eliminate THABr excess, multiple precipitation/isolation steps were carried out from acetonitrile solution upon water addition. Commercially available iron(III) tetrakis (5,10,15,20-mesityl) porphyrin (TMPFeCl), *cis*-cyclooctene and adamantane were used as received without further purification; 1,2-dichloro-ethane (DCE) was purified with H_2SO_4 and then distilled over P_2O_5 according to a literature procedure [16].

2.2. Instrumentation

GC analyses were performed with a Hewlett Packard 5890 Series II instrument, equipped with flame ionization detector and capillary column HP 5 (30 m; i.d. 0.32 mm; 0.25 μm film thickness); GC–MS analyses were performed with Agilent 5973 Network Mass Selective Detector, coupled with Agilent 6850 series GC System equipped with a capillary column Alltech HP-5 (30 m; i.d. 0.32 mm; 0.25 μm film thickness); ^{1}H NMR were recorded on a Bruker AV 300 instrument, equipped with a multinuclear probe spectra; MS (ESI) analyses were performed with a Finnigan MAT LCQ instrument; FT-IR spectra were recorded with a Perkin-Elmer 1600 series instrument; UV–vis spectra were recorded on Perkin-Elmer Lambda 5 and Lambda 16 spectrophotometers.

2.3. Catalytic oxidations

Aerobic oxidations of *cis*-cyclooctene or adamantane were performed in 1,2-dichloroethane (DCE), at 75 °C, under oxygen atmosphere in closed reactors. The reactions were sampled (50 μl) over time and analysed by GC or GC–MS using *n*-decane as internal standard. The reaction mixture was then extracted in sodium bicarbonate phase, and in acidic chloroform. Products were identified by comparison with spectroscopic literature data and by comparison with authentic standards. Chemical yields and conversions were generally determined by quantitative GC analysis. Catalyst stability was assessed by FT-IR after precipitation from the reaction mixture and washing with diethyl ether, or by UV–vis analysis of the reaction solution.

3. Results and discussion

3.1. Synthesis and characterization of iron-substituted polyoxotungstates

Fe-substituted POMs have attracted a great deal of interest, because of the well recognized catalytic properties of iron both in biological and synthetic systems and also due to the existence of straightforward procedures for its insertion into an inorganic POM framework. Indeed, metalation of the mono-lacunary Keggin ion $[\alpha\text{-}SiW_{11}O_{39}]^{8-}$ is achieved in hot water by stoichiometric reaction with $FeCl_3$ [13]. The resulting $[\alpha\text{-}(FeOH_2)SiW_{11}O_{39}]^{5-}$ ($FeSiW_{11}$), after isolation as THA salt, is characterized by FT-IR spectroscopy, showing peaks in the expected region, at 910, 867 and 789 cm^{-1}. The title catalyst can be also characterized in solution by ESI-MS, yielding cluster isotopic distributions centered at 910 and 1030 *m/z*, corresponding, respectively, to $[H_2FeSiW_{11}O_{39}]^{3-}$ and $[(THA)HFeSiW_{11}O_{39}]^{3-}$ anions. In a similar manner, the di-nuclear species $[\gamma\text{-}(FeOH_2)_2SiW_{10}O_{38}]^{6-}$ (Fe_2SiW_{10}) is obtained by metalation of the di-vacant $[\gamma\text{-}SiW_{10}O_{36}]^{8-}$ ligand with two equivalents of $FeCl_3$ [17]. FT-IR and ESI-MS analysis confirmed the expected structure with fingerprint peaks at 960, 903, 808, 756 cm^{-1} and $m/z = 862$ corresponding to $[H_3Fe_2SiW_{10}O_{38}]^{3-}$. Tetra-substituted, Krebs-type polyoxotungstates with the formula $[\beta\text{-}Fe_4(H_2O)_{10}(XW_9O_{33})_2]^{n-}$ ($Fe_4X_2W_{18}$ with $X = Se^{IV}$, Te^{IV} $n = 4$; $X = As^{III}$, Sb^{III}, $n = 6$) are prepared either by stoichiometric reaction of two α-B-$[XW_9O_{33}]^{9-}$ units with 4 $Fe(NO_3)_3$ in acidic medium [15,18], or by direct reaction of $Fe(NO_3)_3$ with Na_2WO_4 and the hetero atom precursor in acidic condition [15]. The four isostructural polyoxotungstates, isolated as THA salts, show FT-IR spectra with distinctive features in the region of W–O stretching (1000–500 cm^{-1}), and a remarkable enhanced resolution with respect to Cs^+ salts reported previously (Fig. 1) [15].

3.2. Aerobic oxidation of cis-cyclooctene catalyzed by iron substituted polyoxotungstates

Cis-cyclooctene is typically used as a model substrate for alkene epoxidation, as the process occurs with moderate to high selectivity even under auto-oxidation conditions [19]. This

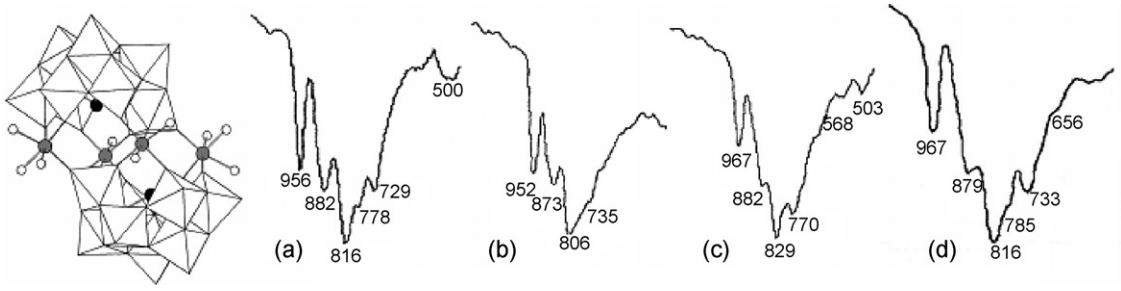

Fig. 1. Structure and FT-IR spectra (1000–500 cm^{-1}) of $[\beta\text{-}Fe_4(H_2O)_{10}(XW_9O_{33})_2]^{n-}$. (a) $Fe_4Sb_2W_{18}$ (b), $Fe_4Se_2W_{18}$ (c), $Fe_4Te_2W_{18}$, and (d) $FeAs_2W_{18}$.

Table 1
Cis-cyclooctene aerobic epoxidation catalyzed by Fe-POMs[a]

#	Catalyst (μmol)	Conversion (%)[b]	Epoxide yield (%)[c]	Selectivity (%)[d]	Induction time (h)	TON[e]	TOF (h^{-1})[f]
1	–	28	16	57	255	–	–
2	$SiW_{12}O_{40}^{4-}$ (0.75)	25	20	80	240	960	16
3	$Fe_4As_2W_{18}$ (0.19)	51	30	59	95	5684	43
4	$Fe_4Sb_2W_{18}$ (0.19)	68	42	62	75	7958	50
5	$Fe_4Se_2W_{18}$ (0.19)	40	25	63	170	7200	46
6	$Fe_4Te_2W_{18}$ (0.19)	58	38	66	105	4737	48
7	$FeSiW_{11}$ (0.75)	46	27	59	135	1296	8
8	$FeSiW_{11}$ (1.50)	68	39	57	100	936	4
9	$FeSiW_{11}$ (3.00)	67	27	40	60	324	2
10	TMPFeCl (0.75)	78	44	56	40	2112	9
11[g]	Fe_2SiW_{10} (1.50)	32	21	65	120	2660	20

[a] In all reactions: DCE 800 μl, *cis*-cyclooctene (3.6 mmol), $T = 75\,^{\circ}C$, $PO_2 = 1$ atm, reaction time = 300 h. POMs are introduced as THA salts.
[b] % of substrate conversion.
[c] Based on substrate.
[d] % epoxide selectivity based on substrate conversion.
[e] Total turnover number (TON): epoxide (mmol)/catalyst (mmol).
[f] Highest turnover frequency calculated as TON per hour on the linear kinetic phase.
[g] DCE 1.5 ml/CH_3CN 0.1 ml, *cis*-cyclooctene (19 mmol), $T = 83\,^{\circ}C$, $PO_2 = 1$ atm, reaction time = 300 h.

benchmark transformation was then exploited to investigate the catalytic activity of the different Fe-substituted polyoxotungstates for aerobic epoxidation. Data in Table 1 allow to evaluate the performance of the Fe-POM catalysts with respect to: (i) the uncatalyzed process (entry 1); (ii) the non-substituted POM complex (entry 2); (iii) structural/electronic factors (entries 3–6); (iv) iron loading (entries 7–9); (v) the iron porphyrin analogue, TMPFeCl (entry 10).

In most reactions the catalyst concentration has been adjusted according to the Fe content in order to provide the system with an overall iron concentration of 0.58 mM. Oxidation of *cis*-cyclooctene leads to the formation of the epoxide as the main product, with selectivity up to 66% for olefin conversion in the range 30–78% after 300 h [20]. In particular, higher selectivity is registered at lower conversion and with a low catalyst loading (compare entries 7–9 in Table 1). In general, the selectivity of the oxidation is not significantly affected by the nature of the Fe-catalyst.

Biphasic, mirror-like traces are obtained for both olefin conversion and product evolution over time, as exemplified in Fig. 2.

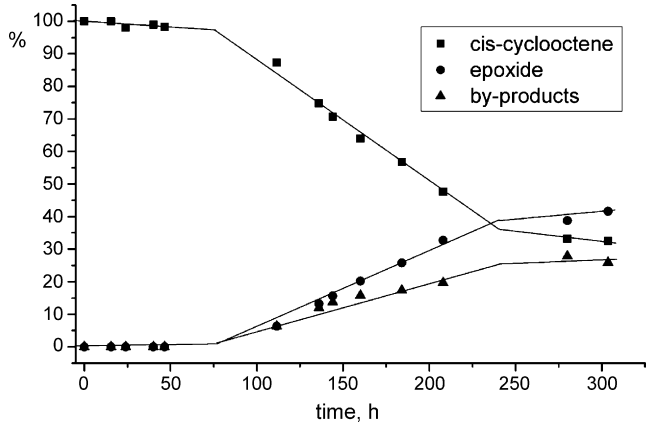

Fig. 2. *Cis*-cyclooctene aerobic epoxidation by $Fe_4Sb_2W_{18}$ (entry 4 in Table 1).

Such kinetic profile is typical of autocatalytic reactions, showing an initial lag time (induction period) followed by a zero-order regime (full chain steps). Therefore, catalyst evaluation and process optimization can be based on two main parameters, i.e. induction time, connected to the initiation phase of the catalytic oxygenation, and turnover frequency (TOF) measured from the fastest linear phase of the kinetics (see Table 1) [21]. In this respect, both the iron-free reactions (entries 1 and 2) show induction times >200 h. On the contrary, iron based catalysts promote the oxidation leading to halved induction times and TOFs in the range 4–50 h^{-1}. Inspection of the catalytic activity displayed by the four isostructural Krebs complexes (entries 3–6) sheds light on the role of the iron center. The nature of the catalyst has a major influence only on the induction time of the oxidation, while the TOF values are basically unaffected, between 43 and 50 cycles/h. In particular, a faster initiation is promoted by $Fe_4Sb_2W_{18}$ and $Fe_4As_2W_{18}$ (induction time < 100 h). The same reactivity trend was observed also in the aerobic auto-oxidation of cyclohexane [7], likely related to their higher reduction potentials [15], thus suggesting that the catalyst is participating in Haber–Weiss chemistry with peroxidic intermediates (see further discussion). The Fe dependence on both the initiation and propagation rate was studied in the case of the mononuclear $FeSiW_{11}$ (entries 7–9). It turned out that, while the propagation rate was basically unchanged, a major effect can be distinguished in the induction time, being 60, 100, 135 h, respectively, with 3.00, 1.50, 0.75 μmol of $FeSiW_{11}$. Indeed, a linear relationship is obtained by plotting the reciprocal of the induction time, correlated to the initiation rate [22], as a function of the catalyst concentration (Fig. 3). The observed linearity suggests a direct involvement of the Fe-catalyst in the initiation process, likely with a first-order dependence [22]. Moreover addition of benzoyl peroxide as a radical initiator causes the complete disappearance of the induction time while leaving unaffected the subsequent propagation rate [23].

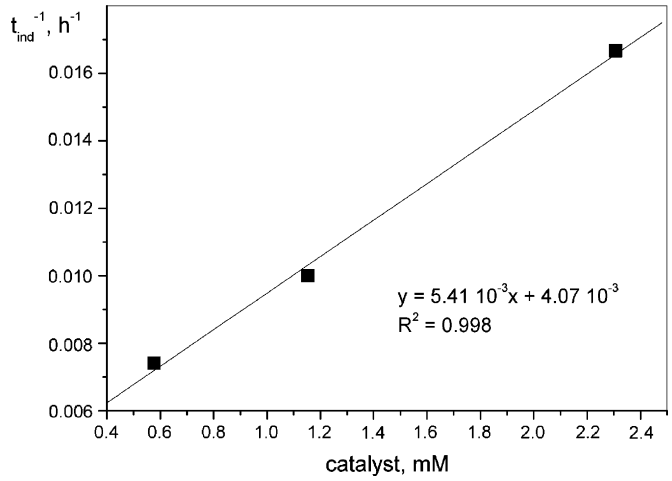

Fig. 3. Linear dependence of the induction time reciprocal on $FeSiW_{11}$ in the aerobic oxidation of cis-cyclooctene (entries 7–9 in Table 1).

The α-Keggin mono-lacunary polyoxotungstates are often considered as inorganic porphyrin analogues due to the geometry of the binding site, providing a planar tetradentate coordination arrangement similar to heme ligands. A direct comparison of the catalytic activity of $FeSiW_{11}$ with FeTMPCl is given in Table 1 (entries 7 and 10). Again a remarkable difference is registered only for the induction time of the oxidation, which is sensibly reduced in the presence of the organic porphyrin (40 h instead of 135 h).

The fate of the porphyrin catalyst can be conveniently monitored by UV–vis spectroscopy in the region of the Soret absorption (418 nm). At the turnover regime, a progressive bleaching of the TMP ligand is observed. Most noticeably, the oxidative degradation follows an autocatalytic behavior in close correspondence with the epoxide formation (Fig. 4). The acceleration of the initiation phase is likely due to the involvement of the organic ligand in the auto-oxidation chain.

On the contrary, the stability of $FeSiW_{11}$ was assessed by FT-IR analysis performed after precipitation of the catalyst at

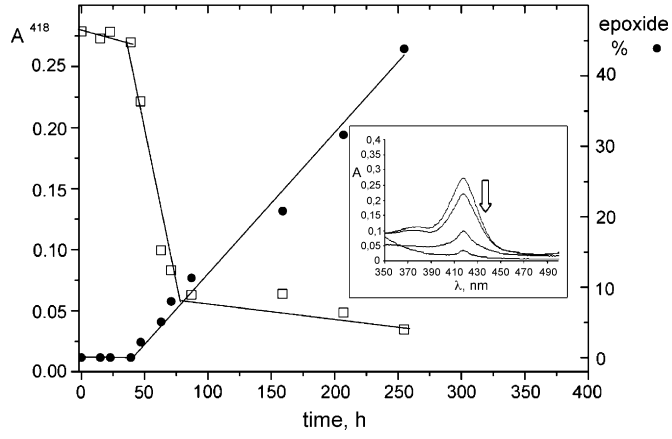

Fig. 4. Aerobic epoxidation of cis-cyclooctene by FeTMPCl (entry 10 in Table 1). Curves over time for: epoxide formation (black circles); TMP bleaching (empty squares) as monitored by UV–vis absorbance at 418 nm, in the Soret band region (inset).

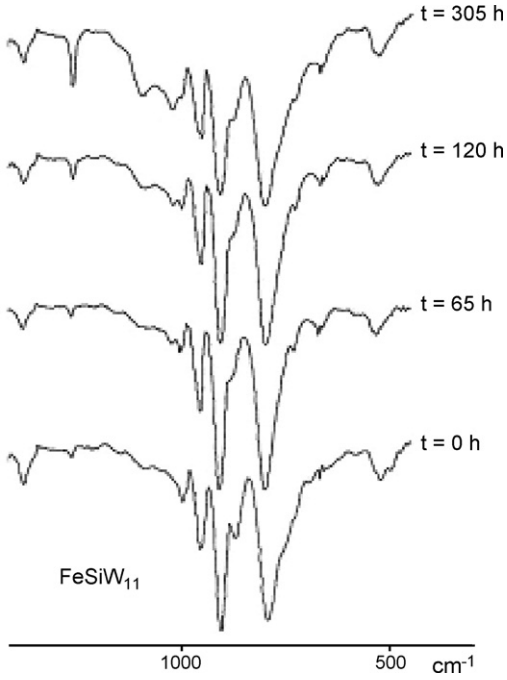

Fig. 5. Infrared absorption of $FeSiW_{11}$ at turnover regime.

different time intervals. As shown in Fig. 5, the POM structural features are preserved despite the prolonged heating.

Analogous conclusions can be drawn for the Krebs-type complexes, where only a modest shift of the W–O stretching absorptions at higher frequencies is observed. A noticeable exception is the dinuclear Fe_2SiW_{10}, used as THA salt in our study [24], which undergoes a major rearrangement of the POM structure as evidenced by a modification of the absorption bands, both in number and intensity, in the region of 1000–700 cm^{-1}. This latter observation together with its reactivity performance appears contradictory with what reported for the TBA salt [24]. However, the central effect of the counterion on the polyoxoanion stability as well as on the energies and rates of electron transfer by POMs, has been highlighted in the literature and might be at the origin of the observed discrepancy [25,26].

To gain further mechanistic evidence on oxygenation catalysis by Fe-POMs, the hydroxylation of adamantane was tested under analogous conditions for two representative Krebs-type catalysts (Table 2).

In particular the selectivity ratio determined from the attack at the tertiary over secondary C–H bonds, on a per H-atom (C_3/C_2), provides valuable information on the nature of the competent oxidant [27]. Therefore, the iron-mediated oxidative chain is also probed by the results of Table 2, according to the following points: (i) the uncatalyzed reaction does not proceed; (ii) products deriving from C–H tertiary attack, 1-adamantanol (1-OH) and 1-chloroadamantane (1-Cl) are observed together with adamantanone (2-one) and 2-chloroadamantane (2-Cl), yielding a selectivity factor C_3/C_2 of ca. 16, a value that falls within the expected range for radical reactions (C_3/C_2 = 1–25) and is similar to those exhibited by analogous porphyrin catalysts (6–10) [28]; (iii) the presence of chlorinated products, are consistent with a radical auto-oxidation mechanism involving the solvent.

Table 2
Aerobic oxidation of adamantane catalysed by iron substituted polyoxometalates[a]

#	Catalyst	Conversion (%)	Product distribution (%)			C_3/C_2	TON[b]	TOF (h^{-1})[c]
			1-OH	1-Cl	2-one + 2-Cl			
1	–	–	–	–	–	–	–	–
2	$Fe_4As_2W_{18}$	54	69.2	15.4	15.4	16.5	162	0.6
3	$Fe_4Te_2W_{18}$	40	68.4	15.8	15.8	16.0	120	0.5

[a] Reaction conditions: DCE 800 μl, adamantane 3.0 mmol, $T = 75\,^{\circ}C$, $PO_2 = 1$ atm, reaction time = 300 h.
[b] % of substrate conversion.
[c] Based on substrate.

4. Conclusions

In our study, catalytic epoxidation by different structural type Fe-POMs with oxygen has been found to occur via radical pathways. The marked dependence of the induction time on the catalyst loading indicates a major role of the iron complex in initiating the auto-oxidation chain. However, the unmatched stability of POM-based ligands under turnover regime, together with the high variety of their structural motifs, makes this class of complexes extremely appealing as oxidation catalysts.

Acknowledgements

Financial support from the Italian National Research Council (CNR) and MIUR is gratefully acknowledged. We also acknowledge ESF COST D29 and D26 actions. This research project has been financed in the frame of FIRB "CAMERE RBNE03JCR5".

References

[1] T. Punniyamurthy, S. Velusamy, J. Iqbal, Chem. Rev. 105 (2005) 2364.
[2] J.-E. Backvall (Ed.), Modern Oxidation Methods, Wiley-VCH Verlag GmbH&Co. KgaA, Weinheim, 2004.
[3] "Polyoxometalates" Special Issue C.L. Hill (Ed.), Chem. Rev. 98 (1998) 1–387.
[4] M.T. Pope, A Muller Polyoxometalate Chemistry. From Topology Via Self-assembly to Applications, Kluwer Academic Publishers, Dordrecht, The Netherlands, 2002.
[5] C.L. Hill, C.M. Prosser-McCharta, Coord. Chem. Rev. 143 (1995) 407.
[6] A. Bagno, M. Bonchio, A. Sartorel, G. Scorrano, Eur. J. Inorg. Chem. 17 (2000), and references therein.
[7] M. Bonchio, M. Carraro, G. Scorrano, U. Kortz, Adv. Synth. Catal. 347 (2005) 1909.
[8] M. Bonchio, M. Carraro, A. Sartorel, G. Scorrano, U. Kortz, J. Mol. Catal. A: Chem. 251 (2006) 93.
[9] Y. Nishiyama, Y. Nakagawa, N. Mizuno, Angew. Chem. Int. Ed. 40 (2001) 3639.
[10] N. Mizuno, C. Nozaki, T. Hirose, M. Tateishi, M. Iwamoto, J. Mol. Catal. A: Chem. 117 (1997) 59.
[11] N. Mizuno, M. Hashimoto, Y. Sumida, Y. Nakagawa, K. Kamata, in: T. Yamase, M.T. Pope (Eds.), Polyoxometalate Chemistry for Nano-composite Design, Kluwer Academic/Plenum, New York, 2002, pp. 197–203.
[12] R. Neumann in Ref. [2], Chapter 8, p. 223.
[13] C. Brevard, R. Schimpf, G. Tournè, C.M. Tournè, J. Am. Chem. Soc. 105 (1983) 7059.
[14] C. Nozaki, I. Kiyoto, Y. Minai, M. Misono, N. Mizuno, Inorg. Chem. 38 (1999) 5724.
[15] U. Kortz, M.G. Savelieff, B.S. Bassil, B. Keita, L. Nadjo, Inorg. Chem. 41 (2002) 783.
[16] D.D. Perrin, W.L.F. Armarego, D.R. Perrin, Purification of Laboratory Chemicals, 2nd ed., Pergamon Press, Oxford, 1980.
[17] J. Canny, A. Tèzè, R. Thouvenot, G. Hervè, Inorg. Chem. 25 (1986) 2114.
[18] Isomerisation of the α-B-$[XW_9O_{33}]^{9-}$ to β-$[XW_9O_{33}]^{9-}$ unit is observed during the metalation.
[19] D.E. Van Sickle, F.R. Mayo, R.M. Arluck, J. Am. Chem. Soc. 87 (1965) 4824.
[20] The allylic oxidation product 1-cyclooctene-2-one was detected only in traces by GC–MS analysis. Other by-products were identified as mainly carboxylic acids. The reaction mixture presents ^{1}H NMR signals between 2.1 and 2.7 ppm, indicative of methylene groups bound to carboxylic functions and whose integration accounts for the mass balance of the oxidation.
[21] Even though the multi-step auto-oxidation mechanism is hardly described by TON and TOF macro-parameters, they might provide straightforward guidelines for process optimisation.
[22] M. Bonchio, V. Conte, F. Di Furia, G. Modena, S. Moro, J.O. Edwards, Inorg. Chem. 33 (1994) 1631.
[23] Reaction 7 in Table 1 was performed also in the presence of benzoyl peroxide (7.6 μmol).
[24] At variance with the literature report [9], in our hands the tetrabutylammonium salt was not completely soluble in the reaction system (entry 11 in Table 1). The oxidation catalyzed by the THA salt occurred with similar TOF, but with induction time >120 h, and selectivity around 75% (entry 11 in Table 1).
[25] V.A. Grigoriev, D. Cheng, C.L. Hill, I.A. Weinstock, J. Am. Chem. Soc. 123 (2001) 5292.
[26] V.A. Grigoriev, C.L. Hill, I.A. Weinstock, J. Am. Chem. Soc. 122 (2000) 3544.
[27] M. Bonchio, G. Scorrano, P. Toniolo, V. Artero, A. Proust, V. Conte, Adv. Synth. Catal. 344 (2002) 841, and references therein.
[28] F. Minisci, F. Fontana, S. Araneo, F. Recupero, S. Banfi, S. Quici, J. Am. Chem. Soc. 117 (1995) 226.